Journal of the Iranian Chemical Society (2018) 15:1527–1534
https://doi.org/10.1007/s13738-018-1350-y

ORIGINAL PAPER

Ag nanoparticles for determination of bisphenol A by resonance light-scattering technique

Masoumeh Pirdadeh-Beiranvand[1] · Abbas Afkhami[1] · Tayyebeh Madrakian[1]

Received: 29 October 2017 / Accepted: 19 March 2018 / Published online: 23 March 2018

Abstract
Resonance light-scattering (RLS) technique was developed for studying the interaction of silver nanoparticles (Ag NPs) with bisphenol A. A simple and environmentally friendly method was developed to synthesize Ag NPs using cinnamon extract. Synthesized nanoparticles were characterized using various measurement techniques. The synthesized Ag NPs were nearly spherical, with the sizes ranging from 30 to 60 nm. Spectral analysis indicated that the cinnamon extract acted as the reducing and capping agents on the surface of Ag NPs. RLS technique was used as the detection method. Light-scattering properties of the synthesized nanoparticles in the presence or absence of bisphenol A was selected as the detection signal. Under the optimal conditions, the linear dynamic range and RSD were found to be 0.01–10.0 mg L^{-1} and 2.78% ($n = 3$), respectively. A limit of detection of 0.005 mg L^{-1} was obtained for the determination of bisphenol A. The obtained results showed successful application of the method for the analysis of bisphenol A in real samples.

Keywords Silver nanoparticles · Bisphenol A determination · Resonance Rayleigh scattering · Cinnamon extract · Baby milk bottles · Milk

Introduction

Bisphenol A (4,4'-dihydroxy-2,2-diphenylpropane, BPA) is used as a monomer in manufacturing most polycarbonate plastics and epoxy resins. The products are used in baby bottles, as protective linings for canned foods and beverages, and also as a coating on metal lids for glass jars and bottles. These uses result in consumer exposure to BPA via the diet. BPA is a hormone-disrupting chemical that in animal studies has been associated with reproductive abnormalities such as lower sperm counts, enlarged prostate glands, hormonal changes, and precancerous changes in the breast and prostate. The increasing global concern over BPA exposure highlights the importance of developing analytical methods to detect traces of this compound in environmental samples [1–3].

In recent years, many analytical methods involving liquid chromatography–mass spectrometry (LC–MS) [4], high-performance liquid chromatography (HPLC) [5], and gas chromatography–mass spectroscopy (GC–MS) [6] have been adopted for the determination of BPA in real samples. However, these methods suffer from several disadvantages such as the high price of instruments and time-consuming sample pre-treatments and/or use of large amounts of toxic organic solvents which may be dangerous to human health and the environment. Thus, development of an accurate and rapid method for sensitive and selective detection of BPA is very important [7–9].

Since the pioneering work of Pasternak et al. [10] on resonance light-scattering (RLS) spectroscopy, this method has received notable attention. It is interesting to note that RLS method is an effective approach which overcomes the disadvantages of other current methods [7]. RLS has emerged as a powerful optical technique based on the elastic light scattering [11–14]. By coupling and scanning simultaneously excitation and the emission monochromators of a common spectrofluorometer, enhanced RLS signals could be obtained. The enhanced RLS signals could be used for designating biological macromolecules, aggregation species, and analytical purposes. Due to the advantages of rapidness, high sensitivity, simplicity, and convenience (using a common spectrofluorometer), RLS has attracted much more attention of analytical physicists and chemists [15].

✉ Abbas Afkhami
afkhami@basu.ac.ir

[1] Faculty of Chemistry, Bu-Ali Sina University, Hamedan 65178-38695, Iran

Recently, RLS has been applied for the determination of inorganic ions [16, 17], proteins [18], nanoparticles [19], and drugs [11]. RLS is shown to be a sensitive and selective method for studying electronics-coupled chromophore arrays. RLS is an elastic scattering and very sensitive to the interaction caused by weak binding forces such as intermolecular electrostatic attraction, hydrophobic interaction, and aggregation interaction of biological macromolecules [14].

Due to the unusual optical properties of nano-Ag and nano-Au (which is related to their ability in supporting surface plasmons), these nanoparticles are extremely used in RLS studies. Silver exhibits many advantages such as sharp absorption bands, high absorptivity, high ratio of scattering to absorbance, and extremely high field enhancements, and as they have the same scale with biological proteins, macromolecules and nucleic acids, they are particularly suitable for biological sensing [20, 21]. In analogy to Au nanoparticles, Ag nanoparticles of the same size possess much higher extinction coefficients that cause sensitive detection with minimal material consumption [7].

Nanoparticles (NPs) can be produced by many chemical and physical methods [22, 23]. But some chemical methods use toxic chemicals as stabilizing agent and reducing agent, organic solvents or nonbiodegradable agents. For the synthesis of metal NPs to be used for biomedical, dentistry, clothing, and catalysis applications, there is an increasing need to develop eco-friendly process without any toxic chemicals. Hence, the development of a simple, cost-effective process and green synthesis of AgNP using microorganisms or plants is of great importance. Reducing and stabilizing abilities of natural plants extracts came directly from various constituents containing $–NH_2$, –COOH, –OH, –SH, etc., groups.

In this paper, we used light-scattering properties of Ag NPs for the determination of BPA. A cinnamon extract solution was used as a reducing and capping reagent for the Ag NPs synthesis in the distilled water as the reaction medium [24]. RLS was used as the detection method. The magnitude of RLS intensity was obtained from the synchronous scanning at $\lambda_{ex}=\lambda_{em}$ ($\Delta\lambda=0$ nm). The change in RLS intensity (ΔI_{RLS}) was obtained by measuring the difference between the assay system (I_{RLS}) and the reagent blank (I_0) at 454 nm, namely $\Delta_{RLS}=I_{RLS}-I_0$.

Experimental

Apparatus

The RLS spectra and the intensity of RLS were measured with a Perkin Elmer (LS50B) luminescence spectrometer with a 1.0-cm quartz cell, slit width of 10 nm, and wavelength scan rate of 500 nm min^{-1}. The magnitude of RLS intensity was obtained by the synchronous scanning at $\lambda_{ex}=\lambda_{em}$ ($\Delta\lambda=0$ nm). The RLS intensity change (ΔI_{RLS}) was obtained by the difference between the assay systems (I_{RLS}) and the reagent blank (I_0) at 454 nm, namely $\Delta I_{RLS}=I_{RLS}-I_0$. A Metrohm model 713 pHmeter was used for the pH adjustments. A 40-kHz universal ultrasonic cleaner water bath (RoHS, Korea) was used. The crystal structure of the synthesized materials was determined by an X-ray diffractometer (XRD, 38066 Riva, d/G. Via M. Misone, 11/D (TN) Italy). The morphology, size, and structure of the nanoparticles were characterized by transmission electronic microscopy (TEM, Philips-CMC). The UV–Vis absorbance of the samples was measured using a single-beam UV-mini-WPA spectrophotometer to confirm the formation of Ag NPs.

Reagents and materials

All the chemicals and reagents used in this work were of analytical grade and purchased from Merck Company (Merck, Darmstadt, Germany). BPA was obtained from Sigma-Aldrich (St. Louis, MO, USA). Stock solutions of BPA (1000 mgL^{-1}) were prepared in double-distilled water (DDW) and maintained at 4 °C. Working standard solutions were prepared by suitable dilution of the stock solutions. Britton–Robinson universal buffer was used for pH adjusting of working solutions. Cinnamon powder was obtained from the local markets in Hamedan.

Green synthesis of Ag NPs

Cinnamon extract was used as a reducing agent for AgNP synthesis. For preparation of the extract, 2.0 g of cinnamon powder was dispersed in 100 mL deionized water in a conical flask and boiled for a 20 min and then cooled to room temperature. The dispersion was then filtered to obtain a clear solution of cinnamon extract which was stored in refrigerator at 4 °C. The clear filtered solution of cinnamon extract (1.5 mL) was added to $AgNO_3$ (5 mL, 1 mM) solutions in screw cap vials and stirred at room temperature for 24 h. The solution color changed from yellow to brown with an increase in extract concentration indicating the formation of NPs [24].

General procedure

In a series of 5-mL volumetric flasks, 0.5 mL of 0.8 mg L^{-1} Ag nanoparticle solution, 1.0 mL of pH 6 Britton–Robinson buffer solution, and appropriate volumes of the sample solution were added and diluted to the mark with water. The mixture was ultrasonicated for 5 min. All RLS spectra were obtained by scanning simultaneously the excitation and emission monochromators of spectrofluorometer with the same wavelength from 200 to 800 nm. The intensity of RLS

was measured at 454 nm with silt width of 10 nm for the excitation and emission wavelengths.

Sample preparation and determination

Polycarbonate products (baby milk bottles) were analyzed as the real samples. The products were purchased from local stores in Hamedan. Three replicate experiments for each product were conducted to determine whether BPA was released into the hot water and milk stored in the products. Filled bottles were shaken on an orbital shaker for 1 h at 100 °C [1]. Furthermore, in order to evaluate the method accuracy, all of the polycarbonate products were spiked with BPA at 1.0 mg L^{-1} and 5.0 mg L^{-1} concentration levels.

For the analysis of milk samples, 20 mL of the sample was suspended in 10 mL of water. An appropriate amount of BPA was added, and then proteins were removed from the matrix by adding 2 mL of acetonitrile solution. Finally, after being shaken for 30 s, the sample was centrifuged for 3 min (4000 rpm), and the supernatant was collected [2] and analyzed by the proposed method.

Results and discussion

Characterization of the nanoparticles

The formation of Ag NPs was visually characterized by the color change of the solution, transforming from yellow to dark brown [24, 25]. Figure 1 shows the change in color of the $AgNO_3$ solution with an increase in cinnamon extract concentration, indicating the formation of Ag NPs.

The formation of Ag NPs was further confirmed by the UV–Vis absorption spectra as shown in Fig. 2. UV–Vis absorption spectrum for Ag NPs containing Ag presented

Fig. 1 Photographs of **a** cinnamon extract **b** Ag NPs

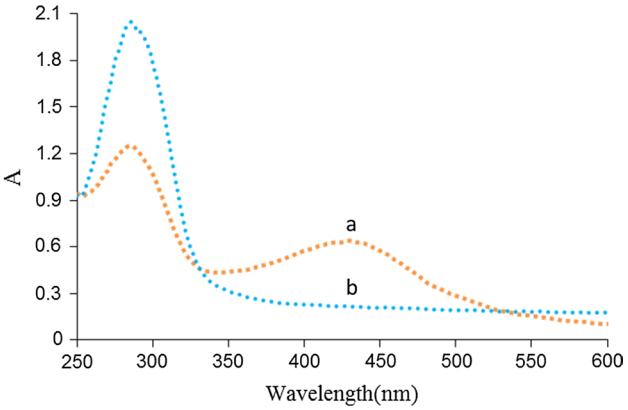

Fig. 2 UV–Vis absorption spectra for **a** Ag NPs and **b** cinnamon extract

a distinct surface plasmon resonance (SPR) absorption at around 422 nm [24].

FTIR spectroscopy measurements were carried out to characterize and identify the functional groups which are bound distinctively on the Ag NPs surface and involved in the synthesis of Ag NPs. Samples for the FTIR analysis were prepared by drying the cinnamon extract taken before and after synthesis of Ag NPs.

The FTIR spectra for Ag NPs indicated the presence of peaks very similar to the ones present in the FTIR spectra of cinnamon extract. This observation indicates that the cinnamon extract acts not only as a reducing agent, but also as a capping agent. As seen from Fig. 3, the spectra for cinnamon extract shows peaks at 1630 and 1700 cm^{-1}, which correspond to stretching vibrations of cinnamaldehyde, a major component of the cinnamon extract. The peaks at 1630 and 1366 cm^{-1} correspond to an aromatic ring and C– OH bending, respectively. Those from 3600 to 3200 cm^{-1} can be assigned to the O–H stretch for alcohols and phenols present in cinnamon [24].

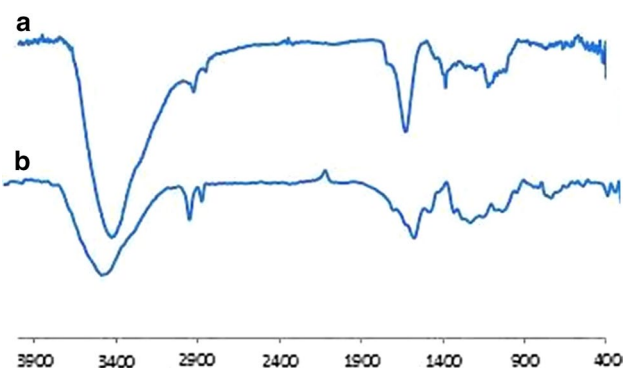

Fig. 3 FTIR spectra for **a** Ag NPs synthesized using cinnamon extract and **b** cinnamon extract

TEM and SEM were employed to characterize the size, shape, and morphology of the synthesized Ag NPs [24, 26, 27] (Fig. 4). The morphology of Ag NPs is nearly spherical. Ag NPs sizes ranged from 30 to 60 nm.

The typical XRD profile of Ag NPs is shown in Fig. 5. The crystallite size was obtained around 15 nm from the XRD pattern according to the Scherrer's equation:

$$D = K\lambda/(b\cos\theta). \quad (1)$$

The equation uses the reference peak width at angle θ, where λ is the wavelength of incident X-ray (1.5418 A), b is the width of the XRD peak at half height, and K is the shape factor, about 0.9 for Ag NPs [22].

The organic compounds in cinnamon extract could attribute to the reduction of $AgNO_3$ and the stabilization of Ag NPs by the surface bound by the organic compounds [24]. Similar observations were noticed in the green synthesis of Ag NPs using plant extract [24–26].

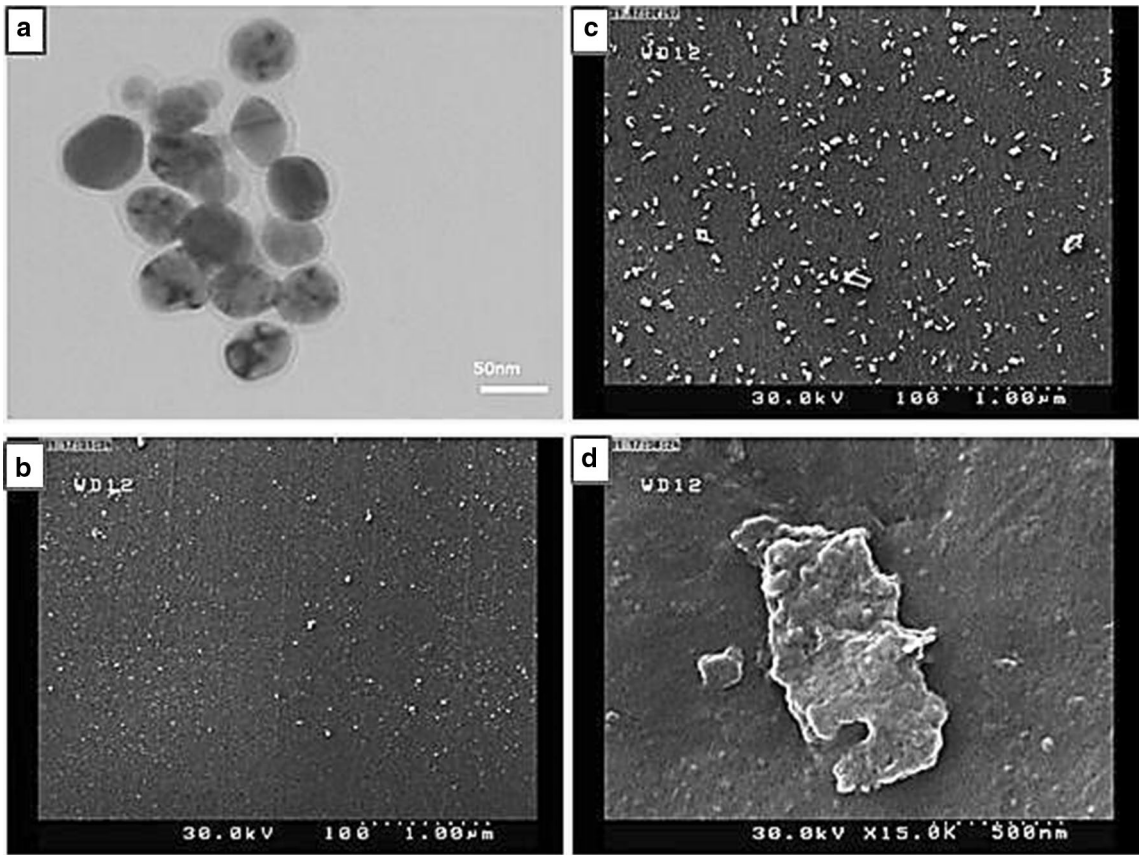

Fig. 4 TEM and SEM images for Ag NPs before and after addition of 1.0 mg. L^{-1} BPA: **a** TEM for Ag NPs synthesized using cinnamon extract, **b** SEM for Ag NPs **c** SEM for Ag NP–BPA and **d** SEM for Ag NPs–BPA

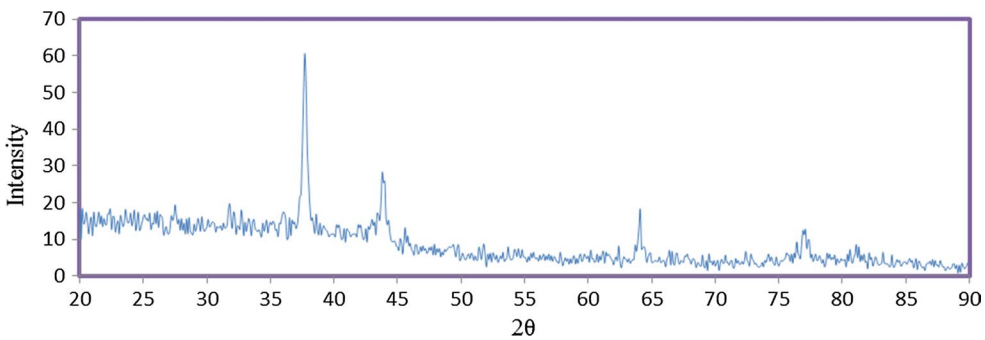

Fig. 5 XRD pattern for Ag NPs synthesized using cinnamon extract

Light-scattering properties of the Ag NP–BPA systems

Figure 6 shows the RLS spectra for Ag NPs and Ag NP–BPA (under optimum condition). As Fig. 6 shows, the RLS spectra for Ag NPs and Ag NP–BPA systems were found to be the same except for RLS intensity. The wavelength of maximum light-scattering (λ_{max}) is located at almost 454 nm for both the investigated systems and their intensities are in the order of Ag NP–BPA > Ag NPs. This is reasonable, because according to the RLS theory [10], the RLS intensity is proportional to r^6 where r is the radius of the particle. When interactions occur between the BPA and Ag NPs, leading to the aggregation of Ag NPs to form bigger volumes of complexes and according to Mie's formalism [28], RLS intensities often increase with the size of the particle. After the addition of analyte, formation of larger complexes results in the increase in the RLS intensities of the system. Overall, the combination of BPA with Ag NPs not only increased the size of the nanoparticles, but also changed their apparent shape (Fig. 4) [27, 29]. The RLS intensity change (ΔI_{RLS}) was obtained by calculating the difference between the assay system (I_{RLS}) and the reagent blank (I_0) at 454 nm, namely $\Delta I_{RLS} = I_{RLS} - I_0$.

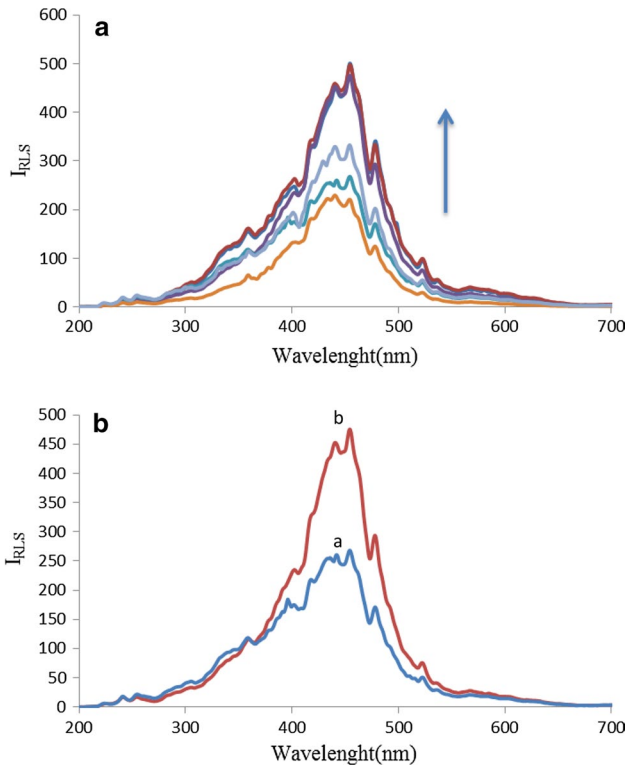

Fig. 6 **A** Effect of various concentration of BPA on RLS spectra of Ag NPs dispersion, increase in BPA concentration from bottom to top. **B** RLS spectra of (*a*) Ag NPs, (*b*) Ag NP–BPA

Effect of pH

The pH of solution plays an important role in the aggregation of Ag NPs and surface binding-sites of the adsorbent. Therefore, the effect of pH on the scattering of Ag NPs in the presence of 1.0 mg L^{-1} of BPA was evaluated in the range 3.0–9.0. The sample solutions were adjusted to the desired pH using 0.1–1.0 mol L^{-1} hydrochloric acid and/or sodium hydroxide solutions. Figure 7 presents the results of the effect of solution pH on the RLS efficiency of BPA. After adding the analyte, the formation of larger complexes between the analyte and Ag NPs results in the increase in the RLS intensities of the system. As Fig. 7 shows, ΔI_{RLS} increased gradually in the pH range 4.0–7.0 and decreased beyond this range. Thus pH 6.0 was selected for future studies for more robustness. The pH_{pzc} for Ag NPs nanoparticles was found to be 5.9. The pH_{PZC} for Ag NPs was determined in degassed 0.01 mol L^{-1} $NaNO_3$ solution at 20 °C. Aliquots of 30 mL of 0.01 mol L^{-1} $NaNO_3$ were mixed with 30 mg Ag NPs in several beakers. The pH of the solutions was adjusted at 3.0, 4.0, 5.0, 6.0, 7.0, 8.0, 9.0, and 10.0 using 0.01 mol L^{-1} of HNO_3 and/or NaOH solutions as appropriate. The initial pHs of the solutions were recorded, and the beakers were covered with parafilm and shaken for 24 h. The final pH values were recorded, and the differences between the initial and final pH (ΔpH) of the solutions were plotted against their initial pH values. The pH_{PZC} corresponds to the pH where ΔpH = 0 [30]. The consecutive pKa values of BPA are 9.6 and 10.2 [31]. The decrease in the RLS signal of BPA at pH > pKa can be due to the electrostatic repulsion between the adsorbate and sorbent.

To maintain the pH of the solution at 6.0, buffer solutions with pH 6.0 such as acetate, phosphate, and Britton–Robinson buffers were examined. It was found that the Britton–Robinson buffer of pH 6.0 was more suitable. Therefore, Britton–Robinson buffer of pH 6 was selected for this study.

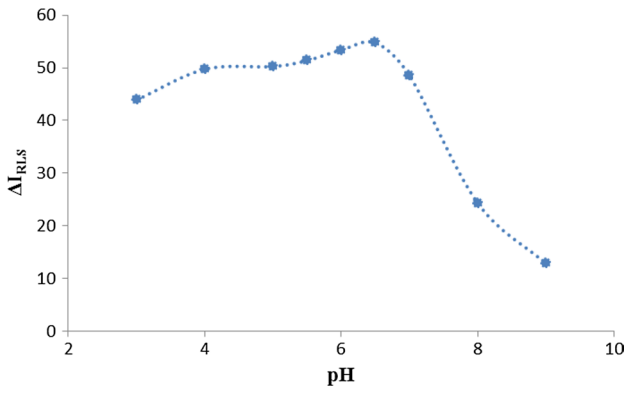

Fig. 7 Influence of the solution pH on the RLS signal intensities. Experimental conditions: ultrasonication time: 1 min, nanoparticle dosage: 0.5 mg L^{-1}, BPA concentration: 1.0 mg L^{-1}

Effect of ultrasonication time

The effect of ultrasonication time on RLS signal was examined at the range 0.0–8.0 min under ultrasonication. The adsorption efficiency was increased by increasing the ultrasonication time up to 3.0 min. After 3.0 min, the RLS signal remained nearly constant. Using effective ultrasonication, nanoparticles agglomeration could be cleaved down by different levels. This factor causes increasing the number of scattering centers and, whereby, a clear augment in scattering signal. On the other hand, much adsorption of BPA on the surface of the Ag NPs leads to the increase in the size of those NPs and finally causes the scattering signal augment. The ultrasonication time profiles indicated that the equilibrium was reached after 3.0 min (Fig. 8). Thus, an exposure time of 5.0 min was selected for the subsequent experiments.

Effect of Ag NPs dosage

The effect of the amount of NPs dosage was investigated by adding Ag NPs in the range 0.1–1.5 mg L^{-1} to the system. The RLS intensity increased by increasing Ag NPs dosage up to 0.5 mg L^{-1} and remained nearly constant at higher concentrations. Also, availability of the surface area of Ag NPs, and whereby signal variations, increased. Therefore, an amount of 0.8 mg L^{-1} Ag NPs was chosen as the optimum amount of Ag NPs in order to achieve maximum signal variation and the highest possible fluorescence intensity. The results are shown in Fig. 9.

Interference studies

The effect of various compounds on the preconcentration and determination of 4.0 mg L^{-1} BPA was studied. The tolerance limit was defined as the amount of the external ion causing an error $< \pm 5\%$ in the determination of BPA. The results are shown in Table 1. The results demonstrate good selectivity of the proposed method and applicability of the method to the accurate determination of BPA in real samples.

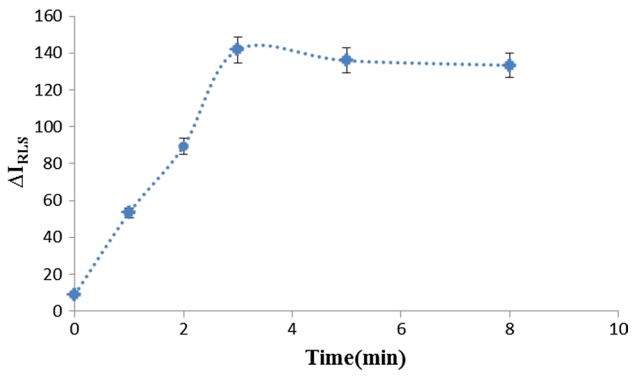

Fig. 8 Influence of the ultrasonication time on the RLS signal intensities. Experimental conditions: pH: 6.0 using Britton–Robinson buffer, nanoparticle dosage: 0.5 mg L^{-1}, BPA concentration: 1.0 mg L^{-1}

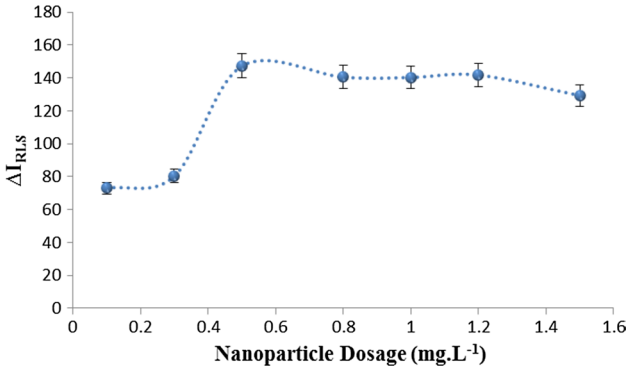

Fig. 9 Influence of the nanoparticle dosage on the RLS signal intensities. Experimental conditions: ultrasonication time: 5 min, pH: 6.0 using Britton–Robinson buffer, BPA concentration: 1.0 mg L^{-1}

Table 1 Interference of some coexisting substances for 4.0 mg L^{-1} of BPA

Interfering species	The tolerable concentration ratios
Ca^{2+}, Na^{+}, K^{+}, Fe^{3+}, NO_3^{-}, Cl^{-}, Mg^{2+}	500
Phenol	100
4-Aminophenol	30

Table 2 Assay of leached BPA from real samples under simulated use conditions

Sample	Spiked (mg L^{-1})	Found[a] (mg L^{-1})	Recovery (%)
Baby milk bottle			
DDW heated	–	0.89 ± 0.03	–
	1.00	1.80 ± 0.09	91.0
	5.00	5.82 ± 0.01	98.4
Milk heated	–	1.23 ± 0.06	–
	1.00	2.17 ± 0.10	94.0
	5.00	5.89 ± 0.12	93.2
Milk			
Brand 1	–	0.06 ± 0.16	–
	1.00	0.90 ± 0.05	84.0
	5.00	4.63 ± 0.13	91.4
	–	0.15 ± 0.01	–
Brand 2	1.00	1.09 ± 0.025	94.0
	5.00	4.78 ± 0.20	92.6

[a]Average of three measurements ± standard deviations

Table 3 Comparison of the proposed method with some previously reported methods for BPA determination

Method	LOD ng ml^{-1}	LDR ng ml^{-1}	Sample	References
MIP/SPE/FL[a]	1.5	5–1000	Plastic cups, toy, and baby milk bottle	[1]
UEME[b]	0.01	0.1–3	Thermal printer paper, toys, and baby utensils	[32]
LLME-CE-UV[c]	4.0	20–2000	Water	[33]
DLLME (GC/MS)[d]	0.03	0.1–5.0	Urine	[34]
RLS	5.0	10–10000	Baby milk bottle, Milk	This work

[a]Molecularly imprinted polymers

[b]Ultrasound-assisted emulsification microextraction

[c]Liquid–liquid microextraction

[d]Dispersive liquid–liquid microextraction

Analytical parameters

The calibration curve was produced from RLS measurements performed under the optimum conditions described above. The calibration curve was linear in the range 0.01–10.0 mg L^{-1}. The calibration equations was $\Delta I_{RLS} = 48.937\ C + 26.345$ with a correlation coefficient of 0.9939 ($n = 9$), where ΔI_{RLS} is the RLS signal change in the presence of BPA at 454 nm and C is BPA concentration in mg L^{-1}. The detection limit (DL) was found to be 0.005 mg L^{-1}. The relative standard deviation (RSD) was found to be 1.09 and 2.78% for 3 and 0.5 mg L^{-1} BPA ($n = 3$), respectively.

Determination of BPA concentration in real samples

The analytical applicability of the proposed method was evaluated by determining the leached BPA from some baby milk bottle and milk samples. The results are listed in Table 2 and show that all of the investigated samples released detectable amounts of BPA into water and milk under simulated use conditions. The results of the spiked samples show good recoveries of the proposed method and suggest that the method is a good candidate for BPA determination in the investigated samples.

Table 3 shows a comparison between the analytical parameters for the present method with those reported for existing methods for the determination of BPA.

Conclusion

A method was presented for the determination of BPA based on its interaction with Ag NPs. RLS method was used as the detection method. The proposed RLS method is simple, rapid, and environmentally friendly for the determination of BPA. The interactions between the BPA and Ag NPs lead to the aggregation of Ag NPs to form bigger volumes of complexes. After adding the analyte, the formation of larger complexes results in an increase in RLS intensities of the system. Advantages of the proposed method are simplicity, low LOD, short ultrasonication time, wide linear range, simple and inexpensive procedure, and environmentally friendly procedure. Due to high stability of Ag NPs in aqueous solutions, the value of RSD in RLS measurements was smaller. The analogy of the obtained results by this method and pervious ones show that the new method is an alternative and can be developed for the determination of the BPA.

Acknowledgements The Bu-Ali Sina University Research Council and Center of Excellence in Development of Environmentally Friendly Methods for Chemical Synthesis (CEDEFMCS) financially supported this work, and the authors acknowledge that for providing financial resource to this work.

References

1. T. Madrakian, A. Afkhami, E. Vanaei, M. Ahmadi, Anal. Methods **7**, 6299 (2015)
2. L. Molina-García, M.L. Fernández-de Córdova, A. Ruiz-Medina, Talanta **96**, 195 (2012)
3. J. Peretz, L. Vrooman, W.A. Ricke, P.A. Hunt, S. Ehrlich, R. Hauser, V. Padmanabhan, H.S. Taylor, S.H. Swan, C.A. Vande-Voort, Environ. Health Perspect. **122**, 775 (2014)
4. N. Dorival-García, A. Zafra-Gómez, A. Navalón, J. Vílchez, Talanta **101**, 1 (2012)
5. K. Inoue, K. Kato, Y. Yoshimura, T. Makino, H. Nakazawa, J. Chromatogr. B **749**, 17 (2000)
6. M. Kawaguchi, K. Inoue, M. Yoshimura, R. Ito, N. Sakui, N. Okanouchi, H. Nakazawa, J. Chromatogr. B **805**, 41 (2004)
7. D. Yao, A. Liang, W. Yin, Z. Jiang, Luminescence **29**, 516 (2014)
8. Z. Mei, H. Chu, W. Chen, F. Xue, J. Liu, H. Xu, R. Zhang, L. Zheng, Biosens. Bioelectron. **39**, 26 (2013)
9. Z. Mei, W. Qu, Y. Deng, H. Chu, J. Cao, F. Xue, L. Zheng, H.S. El-Nezamic, Y. Wu, W. Chen, Biosens. Bioelectron. **49**, 457 (2013)
10. R.F. Pasternack, C. Bustamante, P.J. Collings, A. Giannetto, E.J. Gibbs, J. Am. Chem. Soc. **115**, 5393 (1993)
11. M. Ahmadi, T. Madrakian, A. Afkhami, Anal. Chim. Acta **852**, 250 (2014)
12. Z. Chen, T. Song, S. Wang, X. Chen, J. Chen, Y. Li, Biosens. Bioelectron. **25**, 1947 (2010)

13. Z. Chen, T. Song, Y. Peng, X. Chen, J. Chen, G. Zhang, S. Qian, Analyst **136**, 3927 (2011)
14. F. Fazl, M. Ahmadi, T. Madrakian, A. Afkhami, Sens. Actuators, B **223**, 379 (2016)
15. L. Yu, Y. Zhang, R. Chen, D. Zhang, X. Wei, F. Chen, J. Wang, M. Xu, Talanta **131**, 475 (2015)
16. H. Cao, M. Wei, Z. Chen, Y. Huang, Analyst **138**, 2420 (2013)
17. J. Dong, A. Liang, Y. Luo, Z. Jiang, Arab. J. Chem. (2015). https://doi.org/10.1016/j.arabjc.2015.02.020
18. Z. Chen, J. Liu, Y. Han, Talanta **71**, 1246 (2007)
19. J. Zhu, Y. Wang, L. Huang, Y. Lu, Phys. Lett. A **323**, 455 (2004)
20. H. Jiang, Z. Chen, H. Cao, Y. Huang, Analyst **137**, 5560 (2012)
21. Z. Chen, X. Zhang, H. Cao, Y. Huang, Analyst **138**, 2343 (2013)
22. A. Afkhami, S. Sayari, R. Moosavi, T. Madrakian, J. Ind. Eng. Chem. **21**, 920 (2015)
23. T. Madrakian, A. Afkhami, H. Mahmood-Kashani, M. Ahmadi, Talanta **105**, 255 (2013)
24. R. Moosavi, S. Ramanathan, Y.Y. Lee, K.C.S. Ling, A. Afkhami, G. Archunan, P. Padmanabhan, B. Gulyás, M. Kakran, S.T. Selvan, RSC Adv. **5**, 76442 (2015)
25. K.J. Rao, S. Paria, ACS Sustain. Chem. Eng. **3**, 483 (2015)
26. Y. Zhang, D. Yang, Y. Kong, X. Wang, O. Pandoli, G. Gao, Nano Biomed. Eng. **2**, 252 (2010)
27. H. Parham, S. Saeed, Talanta **131**, 570 (2015)
28. T. Wriedt, Mie theory: a review, in ed. by W. Hergert, T. Wriedt. *The Mie Theory*, vol. 169 of Springer Series in Optical Sciences (Springer, Berlin, Germany, 2012)
29. H. Parham, N. Pourreza, F. Marahel, Talanta **141**, 143 (2015)
30. T. Madrakian, M. Ahmadi, A. Afkhami, M. Soleimani, Analyst **138**, 4542 (2013)
31. Z.J. Tan, F.F. Li, J. Cent. South Univ. **19**, 2136 (2012)
32. P. Viñas, I. López-García, N. Campillo, R.E. Rivas, M. Hernández-Córdoba, Anal. Bioanal. Chem. **404**, 671 (2012)
33. N. Yildirim, F. Long, M. He, H.-C. Shi, A.Z. Gu, Environ. Sci. Technol. **16**, 1379 (2014)
34. S. Cunha, J. Fernandes, Talanta **83**, 117 (2010)